

Theory of nematic comb-like polymers

This article has been downloaded from IOPscience. Please scroll down to see the full text article.

1987 J. Phys. A: Math. Gen. 20 713

(<http://iopscience.iop.org/0305-4470/20/3/033>)

View [the table of contents for this issue](#), or go to the [journal homepage](#) for more

Download details:

IP Address: 129.252.86.83

The article was downloaded on 31/05/2010 at 11:12

Please note that [terms and conditions apply](#).

Theory of nematic comb-like polymers

X J Wang[†] and M Warner

Rutherford Appleton Laboratory, Chilton, Didcot, Oxon OX11 0QX, UK

Received 2 April 1986

Abstract. Comb polymers with semi-flexible main chains and rod-like nematogenic side chains form interesting nematic phases, largely as a consequence of competition between polymer entropy and rod order. We model this competition taking main chains of various stiffness and side groups of various length. Depending on volume fractions, temperature, nematic coupling and stiffness we get one of three nematic phases which we call N_I , N_{II} or N_{III} . We find that at least one component, main or side chain, must be ordered toward a direction, i.e. have a positive order parameter, and the other order parameter can be positive or negative. We identify the molecular trends leading to each possibility.

The theory, in addition to complex phase diagrams, also predicts unusual properties such as anomalous temperature variation of optical anisotropy and molecular conformational changes. The latter, amenable to small angle neutron scattering, shows a prolate (rod-like) form for the main chain dimension in the N_{II} and N_{III} phases where the main chain order parameter is positive. The oblate (disk-like) form, the N_I phase, is examined in some detail.

1. Introduction

Polymer liquid crystals exhibit unusual properties as a consequence of competition between the orientational ordering, imposed by their liquid crystal character, and the drive to maximal entropy common to all chain systems. We here examine this competition in comb systems where the main (polymer) chain has a given degree of stiffness of its own but hinged to it are stiff side groups, the teeth of the comb, with their own mesogenic tendency. Such systems are prime candidates for smectic formation but we discuss this elsewhere (Renz and Warner 1986a) and restrict ourselves to uni-axial nematic phases. Additional competitive features are present for combs since the side group nematic tendency works against that of the backbone unless the molecular hinges are very weak. We identify the competitive influences below and then construct a theory in § 2. In § 3 we discuss our results.

We find three groups of nematic phases according to temperature and molecular structure. Either the main chain or side groups must have a positive order parameter. With one order parameter positive, the other can be positive or negative. We sketch the possibilities in figure 1 in order to fix our ideas. Because of the many influences in this problem and the novelty of the results obtained, we concentrate on demonstrating qualitative features by selecting various combinations of coupling constants, rather than trying to model specific polymers by estimating the molecular parameters. Some

[†] Permanent address: Department of Physics, Tsinghua University, Beijing, China.

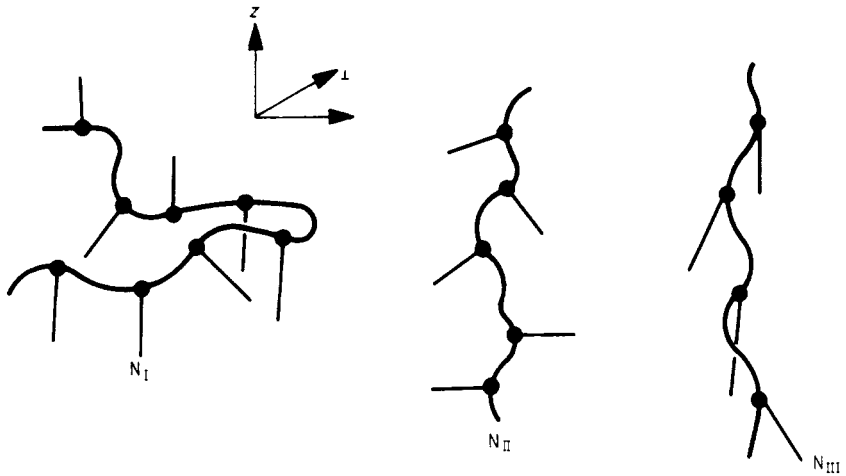


Figure 1. The three principal uniaxial nematic phases possible for comb polymers. The resolution of the five antagonistic tendencies catalogued in the text determines which is stable. N_I ($S_A > 0$, $S_B < 0$; A denoting side and B main chain) has the main chain exploring directions in or close to the plane perpendicular (\perp) to the ordering direction z . The phases N_{II} ($S_A < 0$, $S_B > 0$) and N_{III} ($S_A > 0$, $S_B > 0$) are more reminiscent of the backbone phases since the main chain tangent explores directions about the ordering direction z . All phases are drawn for high degrees of ordering, especially of the main chains.

of the results obtained in § 3 include re-entrant phases and the possibility of the repeated alternation with temperature in the sign of optical anisotropies. In addition, the broad groups identified above are further broken down according to whether or not one of the components suffers a drastic change in order parameter before the nematic–isotropic phase transition. A close analogy with the case of a simple nematic in an external field greater than the critical value is found. We conclude with a discussion in § 4 of existing and further experiments to elucidate the qualitative aspects of liquid crystalline and chain conformations, and their consequences.

In a melt of comb polymers we can identify at least five influences on molecular order which will determine the model to be solved below. These are as follows.

(i) The drive toward parallel order of the mesogenic side chain moieties under the usual influence of steric and soft forces, described by the v_A term in the model, acting between these elements.

(ii) The same nematic influence, v_B , acting between sections of the main chain. This coupling can be weaker than the case of backbone liquid crystalline polymers where the only mesogenic tendency is due to incorporated stiff units.

(iii) The same nematic coupling, v_C , between the directions of the side and main chains tending to make for alignment between them.

(iv) The flexibility of the attachment spacer determining the extent to which side and main chains wish to be perpendicular (coupling v_f). This and (iii) represent the coupling between the molecular components. These two couplings appear together and compete, yielding an overall sign which will alter according to the relative strengths of shape anisotropy and stiffness of the molecular hinge.

(v) The polymeric aspects of the main chain. Here, we have the drive toward maximal entropy in chain conformation on the one hand and the need to reduce bending energy (modulus ϵ) by avoiding highly contorted configurations.

These five requirements are antagonistic to each other. For backbone nematics the transition to an ordered state was seen to be the result of a conflict between orientational order and maximal entropy. The latent entropy of transition is much higher than in conventional nematics indicating the loss to the internal entropy reservoir of the polymer molecules.

For combs conflicts similar to those in backbones can be envisaged. Imagine that the side chains order the most strongly (v_A is large), the most likely situation. Then if v_f dominates over v_C , indicating the need for the main chain to be perpendicular to the side chains (like in a real comb), then the main chain will, on average, be reduced to exploring the plane perpendicular to the ordering direction, an enormous reduction in entropy, though not as great as the restriction to one dimension suffered by the chain in the case of backbone nematics. Because of this additional factor one would expect that mesogenic moieties, when connected by a chain, will have transitions different from when they act independently, as in conventional nematics. We call the above nematic phase N_I .

Another possibility is where mesogenic units in the side chain make v_B comparable to v_A and it is perhaps the main chain that orders with a positive order parameter, S_B , and that it is the side chains that are confined to the perpendicular plane, $S_A < 0$. We call this phase N_{II} . New compounds (Engel *et al* 1985) give hope that these phases N_{II} and N_{III} will be found. This situation would be most conducive to *biaxiality*, a possibility we do not pursue here.

The third alternative, N_{III} , is where v_C dominates over v_f , and the drive toward parallelism of main and side chains due to nematic interactions is stronger than the hinge influence leading to perpendicular orientation. The phase has S_A and $S_B \geq 0$. Figure 1 sketches these three possibilities.

Finally, the coupling to the entropy of chain configurations will have a great effect on chain dimensions in addition to the thermodynamic consequences. The possibilities listed above will lead to an extension of the chain in the perpendicular or parallel directions respectively, the former being an expanded random walk, the latter tending to a rod. There will be a concomitant contraction in the other directions. Small angle scattering experiments, directly probing chain dimensions, are called for as a complement to thermodynamic and optical investigations which have already demonstrated the effects of coupling between main and side chain.

2. A model for comb polymers and its solution

The problem of a worm chain in a nematic field has been reduced to that of the spheroidal wave equation by many authors, first by Jähmig (1979, 1981) and then by ten Bosch *et al* (1983a, b), Warner *et al* (1985) and Wang and Warner (1986a). The latter two papers, hereafter referred to as WGB and ww, show that many aspects of behaviour, especially as order increases, were not available from perturbative approaches. Detailed comparison with experiment is possible (ww).

We employ this method for comb polymers and will use many of the results of WGB and ww. Our approach involves solving simultaneously for the order in the main chain and side chains, analogous to a problem encountered in the problem of a nematic polymer dissolved in a nematic solvent (ten Bosch *et al* 1983b).

We shall work within the mean field approximation. The coupling constants v_A , v_B , v_C and v_f employed here have been discussed in the previous section. Although

it appears to be a purely Maier-Saupe (1959) approach, with the v having the appearance of soft forces, the v incorporate the effect of steric (Flory-Onsager) interactions, and can accordingly have a temperature-dependent component (see WGB).

2.1. Volume fractions and coupling

The relative efficacy of the competing couplings depends partly on the volume fraction of the two components (main chain and side chain). One can envisage altering the balance by either changing

(a) the number of side chains attached per unit length to the main chain, or

(b) the length of side chain elements while keeping constant the number affixed per unit length of main chain.

To allow for either, or both, of the above and to make the effect of moiety length explicit in its effect on both soft and steric forces we follow the approach of Warner and Flory (1980), where the problem of steric effects in thermotropic multicomponent rod systems is examined.

Let the cross sectional dimension l of side chain and main chain be equal for simplicity. Denote the length of side chains divided by this sectional length be x , an axial ratio, and the length of main chain associated with each pendant unit, similarly divided, by n . Then the volume fraction of side chain is

$$\chi = x/(n+x) \quad (2.1)$$

with a maximum possible value of $\chi = x/(x+1)$ when there is one side chain per segment of the main chain, $n=1$. In the results that we shall present, χ is varied at fixed x , i.e. by changing n . One could equally change x , or x and n together. This maximum value of χ at fixed x assumes equal cross sections of side and main chains. Precisely what the maximum χ is will be determined by these relative cross sections and the tacticity of the molecule. In the spirit of looking qualitatively at the types of order possible in response to competing influences we do not pursue the precise nature of the maximum of χ . One can envisage many problems, for instance at high values of χ and for certain tacticities the induction, via steric exclusion effects, of a bottle brush structure to the comb, where side chain freedom is mutually restricted and the main chain becomes effectively stiff. We shall ignore this although it perhaps occurs in a rigid hinge system of Finkelmann and Wendorff (1985) (see our discussion in § 4). This limit of low hinge flexibility, in practice a small number of CH_2 groups in the spacer connecting side to main chain, and high frequency of attachment of side chains, small n , is of great importance since it inhibits nematic phases. The mechanism for inhibition is difficult to model (see our comments below (2.3) on the influence of hinges).

The relative number of side (main) chains seen by a segment (a length of chain equal to its sectional dimension) is then $\chi(1-\chi)$. There is one hinge per side chain irrespective of volume fraction. The mean field potential of a side chain is

$$U_A = -\{\chi v_A x S_A + [(1-\chi)v_c x - v_f] S_B\} P_2(z) \quad (2.2)$$

where v_A and v_B are intersection energies between segments, P_2 is the second Legendre polynomial, $3z^2/2 - \frac{1}{2}$, and $z = \cos \theta_A$. Similarly, the nematic energy of the main chain is

$$U_B = -[(1-\chi)v_B S_B + (\chi v_c - v_f/n) S_A] \int_0^{L_B} ds P_2(\hat{u}_z(s))/l \quad (2.3)$$

where the main chain, of length L_B , is treated as a trajectory in space labelled by the arc position s from one end. The (unit) tangent vector, $\hat{u}(s)$, fulfils the same role as the rod axis for low molecular weight nematics and $u_z(s) \equiv \cos \theta(s)$ with $\theta(s)$ being the angle the tangent vector makes with the ordering direction. The combination of v_c and v_f in the cross coupling clearly demonstrates the competition described in § 1(iv).

2.2. Mean field theory

The appearance of χ and $1 - \chi$ in (2.2) and (2.3) is conventional for mean field theories with soft interactions. These factors merely express the number of neighbours of the appropriate type seen by each segment. For steric interactions, where there is a subtle interplay between shape and volume fraction, the form of the apparent (temperature dependent) potential (compare with Warner and Flory equation (6)) is very different. Expansion of the log yields, for low volume fractions or high degrees of order, forms like (2.2) and (2.3) where \bar{y}/x of Warner and Flory (1980) should be identified with $\langle \sin \theta \rangle$ which is like $1 - S$, approximately. We then assume that (2.2) and (2.3) incorporate steric effects in qualitatively the correct manner.

The influence of one hinge on the tangent of the main chain in (2.3) is considered delocalised over the n segments separating hinges. This is probably reasonable for nl not too much larger than the natural stiffness length of the chain (to be discussed below). Important new classes of materials have been synthesised which include mesogenic elements in the backbone as well (Engel *et al* 1985). The stiffness they imply can make this a good model of delocalised hinge effects. More esoteric phases can be envisaged if nl is larger than the natural stiffness length (Gunn 1985). Each hinge then has a localised effect along the backbone. Also assumed in (2.2) is that a *mean* orientation S_B of backbone is transmitted by the hinge to the side chain, and vice versa in (2.3).

Accompanying the above backbone stiffness between pendant groups is a torsional stiffness implying a correlation between angles consecutive side chains adopt with respect to the ordering direction. The mean field potentials assume they are uncorrelated. The importance of this neglect depends on χ and n . If side chains are relatively far apart on a scale set by their length x then their steric and soft interactions with their neighbours will not mutually interfere. The converse situation, however, could mean that our theory could, for instance overestimate the contribution of side chains to the latent entropy, in this case a property dominated by the backbone. The main chain tangent vector is correlated in any case along the chain by virtue of the backbone stiffness. The most likely effect of side chain correlation is in the side chain contribution to the free energy, something that will perhaps displace transitions in temperature.

The cross coupling influences are weighted by the sizes of side chain and main chain repeat units, x and n . Extracting from the cross coupling the appropriate factors, $x(1 - \chi)$ in (2.2) or χ in (2.3), yields an effective cross coupling $\bar{v}_c = v_c - v_f/(n\chi)$. As Renz (1986) has pointed out to us, if $\bar{v}_c^2 \geq v_A v_B$ then the stationary points in the free energy we find later are no longer minima but saddle points. This mysterious instability when the cross coupling becomes large compared with the self coupling will be taken up elsewhere.

Finally, the finite slope of the *ST* curves as $T \rightarrow 0$ is an artefact of mean field theory. A more accurate low temperature theory (of the spin wave type (see Faber 1977)) would yield zero slope in this limit.

2.3. Excluded volume

In a polymer melt the long range problem of polymer excluded volume is generally unimportant. The dense environment of other chains leads to screening of interactions and the adoption of ideal dimensions. The extension to a rod in the backbone nematic does not enhance the probability of a chain seeing itself. However, a chain in a melt confined to two dimensions by the nematic field, an extreme case for the order envisaged in N_I , cannot for topological reasons be screened and excluded volume statistics must prevail. We ignore this effect here and use ideal (non-excluding) chain statistics. Until the chain is drastically confined to the plane ($S_B \rightarrow -\frac{1}{2}$) we do not expect this to be a serious problem.

2.4. Theory

To obtain the chain partition function we integrate over chain configurations the Boltzmann factor constructed from the mean fields (2.3) and the bending energy of the main chain, with $\beta = (k_B T)^{-1}$:

$$Z_B = \int \delta \hat{\mathbf{u}}(s) \exp\left(-\frac{1}{2}\beta\epsilon \int_0^{L_B} ds \dot{\mathbf{u}}^2(s) - \beta U_B[\hat{\mathbf{u}}(s)]\right). \quad (2.4)$$

As discussed by wGB (2.4) yields an equivalent differential equation for probabilities G of chain configurations allowing evaluation of all averages and Z_B itself. The differential equation represents the diffusion of the tangent vector on the surface of the unit sphere, the rotational diffusion constant $D = (2\beta\epsilon)^{-1}$ yielding an effective step length, D^{-1} , characterising the worm chain persistence in the absence of nematic fields. It is a natural length of chain elasticity in addition to the segmental length, l . It is convenient to reduce main chain lengths by D^{-1} with $s = s'D^{-1}$ and $L_B = ND^{-1}$, whence the first part of (2.4) becomes $-\frac{1}{2} \int_0^N ds' \dot{\mathbf{u}}^2(s')$ and (2.3) becomes

$$U_B = -[(1-\chi)v_B S_B + (\chi v_C - v_f/n)S_A] \alpha \int_0^N ds' P_2(\hat{\mathbf{u}}_z(s)) \quad (2.3')$$

where $\alpha = D^{-1}/l$ is the number of segments in a persistence length, roughly speaking an effective axial ratio for the chain, albeit temperature dependent. The length D^{-1} can be determined by small angle neutron scattering in the isotropic melt phase.

The eigenequation corresponding to the diffusion equation is

$$[\Lambda_n + \nabla_{\hat{\mathbf{u}}}^2 + \Delta^2(1 - \cos^2 \theta)] S p_n(\theta) = 0. \quad (2.5)$$

The angular part only of ∇^2 reminds us that the tangent vector is a unit vector for this length preserving model and that (2.4) represents the diffusion of $\hat{\mathbf{u}}(s)$ on the surface of a sphere with a potential acting. The coupling constant Δ^2 in (2.5) is

$$\Delta^2 = -3\beta\alpha[(1-\chi)v_B S_B + (\chi v_C - v_f/n)S_A]/2. \quad (2.6)$$

In the phase N_I with $S_B < 0$, $S_A > 0$ then $\Delta^2 > 0$, the oblate case, and $\hat{\mathbf{u}}(s)$ is repelled by a polar potential into the equatorial region, i.e. the chain is confined toward the perpendicular plane. For the N_{II} and N_{III} phases with $S_B > 0$ the prolate limit obtains and $\hat{\mathbf{u}}(s)$ is confined to the poles with hair pin transitions between them (an idea of de Gennes (1982); see wGB and ww).

The expression for the Green function $G(\zeta, \zeta_0; N, 0)$ of (2.5) is

$$G(\zeta, \zeta_0; N, 0) = \sum_n \frac{2n+1}{2} S p_n(\zeta) S p_n(\zeta_0) \exp(-\lambda_n N) \quad (2.7)$$

where ζ, ζ_0 are the final and initial values of $\cos \theta$, i.e. u_z , and where $\lambda_n = \Lambda_n + 2\Delta^2/3$. G expresses the probability of starting out at $s' = 0$ with $\zeta = \zeta_0$ and having $\zeta = \zeta$ at $s' = N$.

G gives us averages, for instance the order parameter (w_{GB} (5.18) and w_w (16)) for long chains:

$$S_B = \frac{1}{2} \int_{-1}^1 d\zeta [Sp_0(\zeta)]^2 P_2(\zeta). \quad (2.8)$$

The side chains obey a Maier-Saupe-like theory, albeit with T -dependent couplings, reviewed in this context by w_w . The partition function is (see (2.2)) for U_A

$$Z_A = \int_{-1}^1 dz \exp(-\beta U_A(z)). \quad (2.9)$$

The order parameter S_A is given by

$$S_A = \int_{-1}^1 dz \exp(-\beta U_A(z)) P_2(z) / Z_A. \quad (2.10)$$

Remembering that the right-hand side of (2.8) is determined by Δ^2 , and hence S_A and S_B , it is clear that (2.8) and (2.10) represent self-consistency equations to be solved for S_A and S_B .

Free energies of a side chain and of a whole main chain, at self-consistent values of S_A and S_B , are

$$F_A = -k_B T \ln Z_A - \frac{1}{2} \langle U_A \rangle \equiv x f_A \quad (2.11)$$

$$F_B = -k_B T \ln Z_B - \frac{1}{2} \langle U_B \rangle \equiv N f_B. \quad (2.12)$$

The free energy of a repeat unit is then $x f_A + f_B n l / D^{-1}$ which converts, after division by $(n+x)$, to a free energy per unit volume, f :

$$f = \chi f_A + (1-\chi) f_B / \alpha \quad (2.13)$$

with α , defined after (2.3'), clearly playing the role of an effective axial ratio for the main chain.

In (2.12) Z_B is evaluated by summing over ζ, ζ_0 in (2.7). For long chains the $n=0$ term dominates. The result is as in w_w and involves $a_{0,0}$, the coefficient of P_0 in the expansion of Sp_0 . This is defined in w_w but will not be important for long chains (see (2.15) below). The mean field term in (2.12) involves $\langle \int ds P_2 \rangle$ which becomes $L_B S_B$. Using this and (2.3) one obtains in f_B

$$\langle U_B \rangle / N = \frac{2}{3} S_B \Delta^2 / \beta. \quad (2.14)$$

For the isotropic phase, (2.11)-(2.13) yield $f_1 = -\chi \ln(2)/x - (1-\chi) \ln(2)/\alpha$ which we subtract off all free energies henceforth. The nematic phase free energy relative to the isotropic phase is then

$$\begin{aligned} \beta f_N = & -\chi \ln(Z_A/2)/x + \beta \chi S_A \{ \chi v_A S_A + [(1-\chi) v_C - v_t/x] S_B \} / 2 \\ & + (1-\chi) [\lambda_0 - \ln(a_{0,0}^2)/N] / \alpha - (1-\chi) S_B \Delta^2 / (3\alpha) \end{aligned} \quad (2.15)$$

where, for chains long compared with their persistence length, $N \gg 1$, the $a_{0,0}$ term can be ignored.

2.4.1. Transitions. Comb polymers change phase on the satisfaction of the conditions f_{N_I} , $f_{N_{II}}$ or $f_{N_{III}} = 0$ for the nematic-isotropic transitions and $f_{N_I} = f_{N_{II}}$ for nematic I to II, and analogously to the III phase. There will be an attendant latent entropy, to be evaluated following the derivation of (25) in ww, the only difference being that $\partial\lambda_0/\partial\beta$ is now $4S_B\Delta^2/(3\beta)$. To calculate a molar entropy we immediately meet the problem, discussed in ww under comparison with experiment, of the relation between a persistence length (governing the backbone entropy scale) and a repeat length nl , determining the frequency of occurrence of a side chain. The entropy of a mole of monomers, each comprising a side chain (x units) and n units of main chain, is

$$S_N/R = \ln(Z_A/2) - \beta x S_A \{ \chi v_A S_A + [(1-\chi)v_C - v_f/x] S_B \} - 2n\lambda_0/\alpha + 4n\Delta^2 S_B/(3\alpha) \quad (2.16)$$

where the entropy of the isotropic phase has been subtracted out and terms of order N^{-1} have been ignored. At the transition $f_N = 0$, (2.15) and (2.16) yield for the latent entropy

$$\Delta S/R = -\beta_c x S_A \{ \chi v_A S_A + [(1-\chi)v_C - v_f/x] S_B \} / 2 - n\lambda_0/\alpha + n\Delta^2 S_B/\alpha \quad (2.17)$$

with $\beta_c = (k_B T)^{-1}$ at the transition.

2.4.2. Chain conformations. The antagonistic influences of the nematic field and the internal entropy of the chain are resolved by a distortion of chain statistics away from spherical. In the backbone polymer case (ww) and the N_{II} and N_{III} phases here, with $S_B > 0$, the chain becomes prolate and, in the limit, rod-like. The results of ww for the chain dimensions can be taken over here, with the amended definition of the coupling Δ^2 (equation (2.6)). The N_I phase is different, corresponding to the oblate case of the spheroidal wave equation and with the chain statistics becoming disk-like in the limit (see our proviso about excluded volume). Because of the novelty of chain conformations in the N_I case we examine it in some detail, especially the asymptotics.

For the case of strong nematic order (low temperatures) it is possible to derive simple relations between chain dimensions parallel and perpendicular to the ordering direction, z . The first-order nature of the transition to the N_I phase means there is not a region where the order is arbitrarily small and therefore there is not necessarily a region where a perturbation analysis would be reliable. Proceeding with the strong nematic analysis we note that the result w_{GB} (5.3) for $\langle R_z^2 \rangle$, the mean square dimension in the z direction, depends on the eigenvalue difference $\lambda_{1,0}$. In the strong oblate limit this no longer becomes small (a tunnel splitting) but grows large (Meixner and Schäfke 1954):

$$\lambda_{1,0} = 2\Delta - 1 + O(1/\Delta) \quad (2.18)$$

whereupon, for all polymers (i.e. where $L \geq 1$) the expression for $\langle R_z^2 \rangle$ becomes

$$\langle R_z^2 \rangle = \frac{3}{4} \frac{L_B D^{-1}}{\Delta} \left(\int_{-1}^1 dx Sp_0(x) P_1(x) Sp_1(x) \right)^2. \quad (2.19)$$

The corresponding expression, w_{GB} (5.13), for the mean-square size in the perpendicular plane, $\langle R_{\perp}^2 \rangle = \langle R_x^2 \rangle + \langle R_y^2 \rangle$, reduces to

$$\langle R_{\perp}^2 \rangle = \frac{3}{8} \left(\frac{2L_B D^{-1}}{\lambda_{1,0}^2} \right) \left(\int_{-1}^1 dx Sp_1^1(x) Sp_0^0(x) (1-x^2)^{1/2} \right)^2. \quad (2.20)$$

The difference in eigenvalues tends to a constant:

$$\lambda_{1,0}^1 = \lambda_1^1 - \lambda_0^0 = 1 + 1/2\Delta + \dots \quad (2.21)$$

from which it is clear that (2.20) is only strictly correct for $L_B \gg D^{-1}$. Otherwise the full form of the L dependence of w_{GB} (5.3) must be used.

It remains to evaluate the matrix elements in (2.19) and (2.20). Meixner and Schäfke (1954) give the asymptotic forms of the wavefunctions in the oblate limit in terms of the parabolic cylinder functions. Using these, the matrix elements are $[2/(3\Delta)]^{1/2}$ and $2(1-1/2\Delta)(2/3)^{1/2}$ respectively. The chain dimensions are accordingly

$$\langle R_z^2 \rangle = L_B D^{-1} / [2\Delta^2(1-1/2\Delta)] \quad (2.22)$$

$$\langle R_{\perp}^2 \rangle = 2L_B D^{-1}(1-3/2\Delta) \quad (2.23)$$

and their ratio becomes

$$\langle R_z^2 \rangle / \langle R_{\perp}^2 \rangle = [1/4\Delta^2][1+2/\Delta+\dots]. \quad (2.24)$$

In contrast to the backbone or the N_{II} and N_{III} cases the chain remains a random walk, compressed in the z direction below the isotropic value $L_B D^{-1}/3$ and expanded in the \perp direction above the isotropic value $2L_B D^{-1}/3$ toward the value $2L_B D^{-1}$. The latter result seems paradoxical if one thinks of the random walk having $\frac{1}{3}$ of its steps in each direction and, since it is length-conserving, on complete compression the z steps would be redistributed in the \perp plane giving $L_B D^{-1}$ for this dimension. The resolution lies in the fact that the random walk is on the tangent sphere, not directly in real space. Solving the diffusion equation for a two-dimensional stiff walk, i.e. on the tangent circle, yields the limiting result of $2L_B D^{-1}$. This result we compare with that of Kuhn walks in § 4. Away from the asymptotic limit, just as for the prolate case (ww), one has to solve numerically for the eigenvalues and matrix elements. We shall not address the question of short polymers ($L_B \sim D^{-1}$) in the N_I phase since, in distinction to the prolate case, there is no transition to rod behaviour that can exist for various chain lengths when $T < T_{ni}$.

3. Results

We are interested in a numerical solution of the self-consistency equations (2.8) and (2.10) to give the characteristic order S_A , S_B and phase behaviour via the free energy (2.15) of comb molecules in their four manifestations, N_I , N_{II} , N_{III} and I . It suffices, to show the qualitative features of the phases, to adopt various typical values of the ratio of coupling constants v_A ; v_B ; v_C ; v_f ; ϵ/l , as well as values for two of the quantities n , x and χ , recalling (2.1). We rearrange (2.6) by extracting v_B and denoting, by a prime coupling constant, divided by v_B ,

$$\Delta^2 = -3[(1-\chi)S_B + \chi(v'_C - v'_f/n\chi)S_A] / \tilde{T}^2 \quad (3.1)$$

where the reduced temperature \tilde{T} is

$$\tilde{T}^2 = (k_B T)^2 / (\epsilon v_B / l) \equiv (T/T^*)^2. \quad (3.2)$$

The reduction of temperature follows ww, corresponding to the N_{II} phase at $\chi=0$, at which point Δ^2 in (3.1) would be identical to Δ^2 in ww. The reduction temperature $T^* = (\epsilon v_B / l)^{1/2} / k_B$ defined by (3.2) could be determined by comparison with experiment on N_{II} in the ww limit.

This limit of $\chi=0$ can be achieved either by $x \rightarrow 0$ or $n \rightarrow \infty$. The former limit is pathological in this mean field model because one hinge and its effect on the backbone (see (3.1) and (3.3) below) is associated with each side chain irrespective of the axial

ratio x . The latter limit corresponds to diluting the effect of side chains on backbones, i.e. on Δ^2 (equation (3.1)).

Since in (3.2) the reduction of temperature is by T^* we can equivalently display our results in terms of temperature reduced by the transition temperature T_B of a pure backbone system. we find $T_B = 0.3878 T^*$ so a conversion between the two is easily made. We shall use T/T_B for temperature in our results.

For $\chi \neq 0$ the side chain potential is needed and we extract a factor of v_B from βU_A required in (2.9), yielding after some rearrangement

$$\beta U_A = \frac{-x(v_B/\epsilon l^{-1})^{1/2}}{\bar{T}} [\chi v'_A S_A + (1-\chi)(v'_C - v'_I/n\chi) S_B] P_2(z). \quad (3.3)$$

The pure Maier-Saupe limit of $\chi = 1$ with side chain only is not accessible unless $x \rightarrow \infty$, χ being bounded by $x/(x+1)$. At this point the transition temperature \bar{T}_{N_I} diverges since it is a temperature reduced by backbone parameters $(v_B \epsilon / l)^{1/2}$ whereas the effective side chain nematic coupling xv_A is diverging. We accordingly do not examine this limit.

By selecting various values of the coupling constants we now illustrate the range of behaviour possible for comb polymers as consequences of their molecular architectures. We fix the axial ratio x of the side chains for each case considered and vary the side chain volume fraction χ by varying n , the frequency as we go along the main chain of finding pendant side chains (see (2.1)). We recall at this point the remarks about cross coupling made in the discussion of mean field theory in § 2. Satisfaction of the self-consistency equations (2.8) and (2.10) only yields minima of the free energy (2.15) if $\bar{v}_c^2 < v_A v_B$. For fixed values of the coupling constants, variation of χ will cause \bar{v}_c to vary and hence one must take care with the above inequality. We shall state when, in extreme parts of a phase diagram, values of χ exceed a critical value χ_c and are too large to give reliable results.

3.1. The effect of side chain volume fraction χ on phase type

Figure 2 shows a system which, for different volume fractions χ of side chain, displays all three principal phases N_I , N_{II} and N_{III} and the isotropic phase, denoted by I. Although $\bar{v}_c^2 > v_A v_B$ for $\chi > 0.62$ and there may be instabilities to the right of this point, the general features displayed allow a qualitative discussion of ordering influences. As reduced temperature is raised we have transitions from the N phases to I, proceeding via the primed phases (where one S is small, see discussion of figure 4) or in a re-entrant manner between N_I and N_{II} in a narrow χ region. The phase boundaries between the primed and unprimed phases are shown with broken curves since they are chosen arbitrarily at $|S_A| \leq 0.17$.

General features of the phase diagram can be understood by analysing the competing influences involved in the ordering. At high volume fractions χ of side chain, inspection of the effective potentials (2.2) and (2.3) shows that the ordering of the side chains via their steric (nematic) fields is paramount. Main chains conform to this side chain ordering via their hinge constraints resulting in the oblate N_I phase ($S_B < 0$) found on the right-hand side of figure 2. Conversely, the $S_B > 0$ phases (N_{II} and N_{III}) are found on the left-hand side since there the main chain volume fraction predominates and the free energy must be minimised by choosing the most favourable nematic ordering for main chains. Whether one has N_{II} or N_{III} depends on the balance between side chain shape (x), volume fraction and hinge strength. The effect of the nematic field

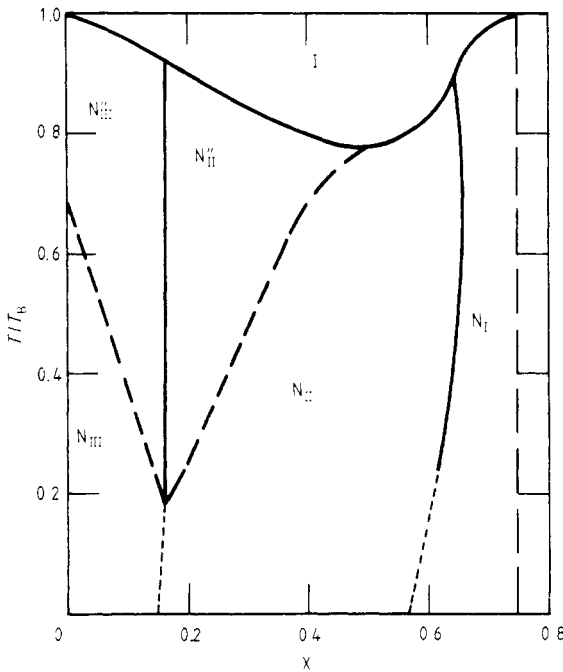


Figure 2. The phase diagram of comb polymers with coupling constants in the ratio $v_A : v_B : v_C : v_f : \epsilon/l = 1 : 2 : 1.2 : 3 : 2$ with the axial ratio of the side chains being $x = 3$. Reduced temperature T/T_B (where T_B is the transition temperature of main chains in the absence of side chains) is plotted against volume fraction χ of side chains up to a maximum value of $\chi = x/(1+x) = 0.75$. The phases N_I , N_{II} and N_{III} are drawn in figure 1 and I denotes the isotropic phase. Broken curves separate the primed N phases from the unprimed at an arbitrary value of $|S_A| \sim 0.17$.

coupling to the side chain shape scales with their length (x) and must be compared with the hinge effect. The dominance of side chain (xv_c) over hinge (v_f) yields N_{III} and vice versa. Here we find N_{III} as $\chi \rightarrow 0$. For finite χ the balance changes and eventually the N_{II} phase appears. This is discussed around equation (3.4). (In figure 3 below we take two values of x and find that each phase diagram has only either N_{II} or N_{III} but not both.) Dotted lines suggest an extension of the phase boundaries to very low temperatures. A more precise analysis will be given elsewhere. The re-entrant part of the phase diagram is in the region $\chi > \chi_c = 0.62$. However we believe re-entrancy to be a general phenomena. An illustration of the variation of properties with temperature at fixed side chain volume fraction, χ , in particular the exchange of sign of the order parameters S_A and S_B , is discussed below in figure 6 where it is shown how optical anisotropy would be a simple test of such phase behaviour.

3.2. The effect of side chain length on phase type

In figure 3(a) we show combs with coupling constant ratios $3 : 2 : 1 : 3 : 2$ and two different axial ratios $x = 5$ and $x = 1$. For the shorter side chains ($x = 1$) the hinge (urging the side chains perpendicular to the main chain) dominates over the nematic field effects and hence only N_{II} and I are found. The phase line terminates at $\chi_c = 0.13$ where the

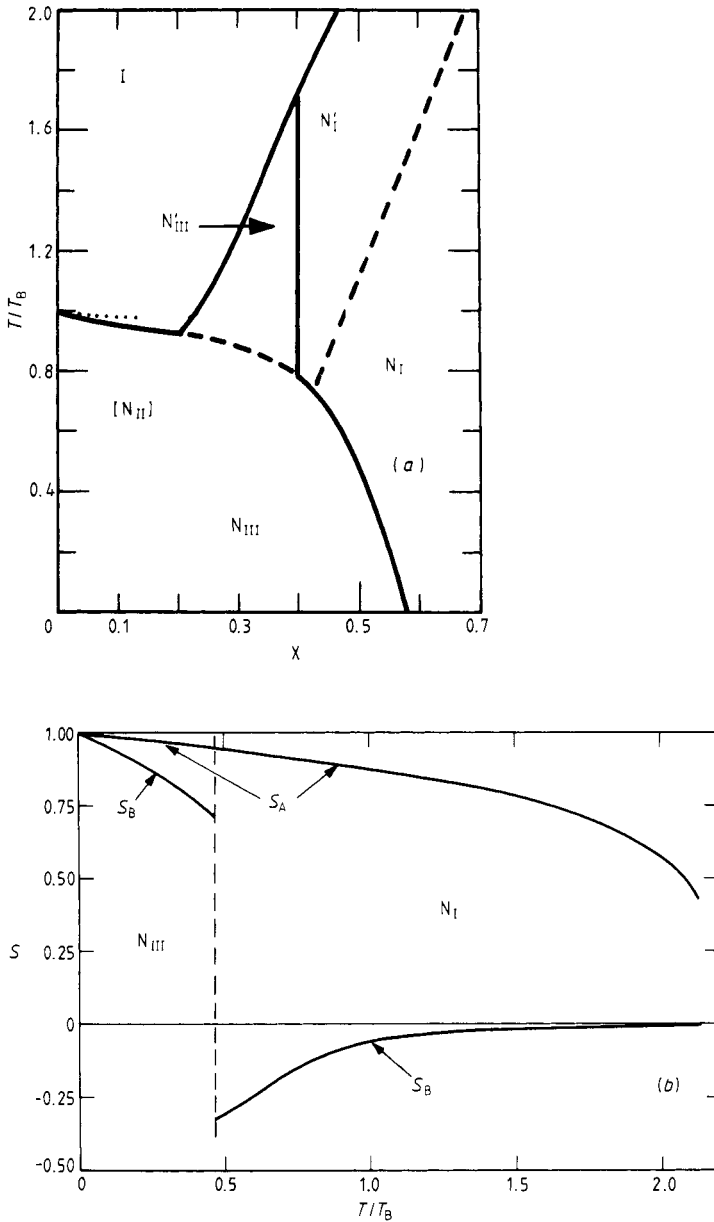


Figure 3. (a) The effect of changing the axial ratio of side chains on the phase behaviour of combs. Reduced temperature T/T_B is shown against side chain volume fraction χ , with maximum possible values of $\chi = 0.5$ for $x = 1$ and $\chi = \frac{5}{8}$ for $x = 5$. Longer side chains ($x = 5$, full and broken curves) lead to N_{III} (side and main chains parallel) when dilute (χ small) and to N_I (the side chains constraining the backbone toward the perpendicular plane, $S_B \leq 0$) when χ is large. The $x = 1$ combs can only support an N_{II} phase (dotted line terminating at $\chi_c = 0.13$), since the hinges are now more effective than a short rod coupling to the nematic field, and an I phase. (b) N_{III} - N_I -I transitions for $x = 5$ combs at $\chi = 0.5$ side chain volume fraction. The main chain order parameter S_B changes sign but, although coupled to the side chains, only a very slight discontinuity in S_A is observed at this reduced temperature $T/T_B = 0.47$ (discontinuity too small to see in the figure at this scale).

effective cross coupling becomes too large. For $x = 5$ the drive for the side chains to respond to the nematic field of the main chain dominates over the effect of the hinge and N_{III} results. As in figure 2, the N_I phases are found (when at all) to the right of the diagram at higher χ . The critical volume fraction limit, χ_c , from the cross coupling, is 0.826, marginally less than the geometric maximum 0.833.

3.3. The primed phases—one order parameter small

The variation of order parameter with temperature for the $x = 5$ side chains of volume fraction $\chi = 0.5$ is shown in figure 3(b) when we have the sequence N_{III} , N_I , N'_I , I involving a change in sign of S_B .

If instead of looking at this volume fraction of side chains we examine $\chi = 0.3$, then we see from figure 3(a) on raising the temperature a phase sequence N_{III} - N'_{III} -I. This is illustrated in figure 4 where the S_B - T curve is reminiscent of that for a nematic in an external field above the critical value (see Wojtowicz and Sheng (1974) for a description of simple nematics in an external field using Maier-Saupe theory and Hornreich (1985) for a Landau theory with refined estimates of critical fields). Here it is the polymer phase that is effectively in an external field (from the A phase). For a genuinely simple backbone polymer the internal degrees of freedom do not qualitatively effect the idea of a line of first-order transitions with a critical endpoint (Wang and Warner 1986b). To see the analogy examine the potentials U_A and U_B ((2.2) and (2.3)). In this case in U_B the v_c and v_f terms are like 'external' fields with magnitude determined by S_A . If the natural transition temperature for B alone, i.e. without the influence of A, is lower than for that of A alone, then above this temperature one essentially has only an $S_B \neq 0$ because of the polarising effect of the field S_A . Figure 4 shows that this temperature, i.e. the point where S_B changes most rapidly with temperature (a memory of the transition), is not quite at $T/T_B = 1$ since (a) there is a reduction because the volume fraction $(1 - \chi)$ of chain is less than 1 and (b) there is an increase, as in the simple polymer case (Wang and Warner 1986b), because of the

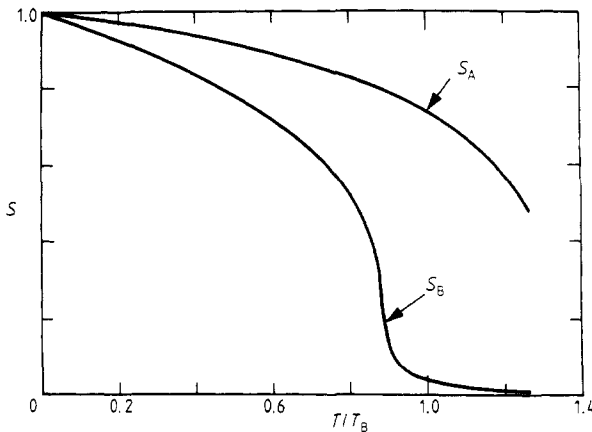


Figure 4. Order parameters S_A and S_B as functions of reduced temperature T/T_B for the transitions N_{III} - N'_{III} -I of the chains in figure 3(a). Volume fraction of side chains is $\chi = 0.3$ and their axial ratio is $x = 5$. Note for S_B the similarity with simple nematics in an external field, here applied by the A component on B. Lack of a discontinuity in S_B implies that we are above the critical field value.

applied field. Our nomenclature for this is N'_{III} , the single prime denoting that it is the B component that resembles a nematic in an external field, i.e. $S_B \sim 0$. If $T_A \leq T_B$ then there is the possibility that $S_A \sim 0$ before the transition to the isotropic phase is achieved. We denote this kind of phase by a double prime, in this case it would be N''_{III} . Figure 2 is now easier to understand, especially the appearance of " phases N''_{II} and N''_{III} . Side chain nematic coupling is relatively weak compared with the relevant backbone parameters and one must examine $(v_B \epsilon / l)^{1/2} : v_A x = 2 : 15$, whereupon T_A is lower than T_B and the A component effectively feels an external field from the B component with a resultant " phase. Contrast this with figures 3(a) and 4 where the corresponding ratio is 2:3, T_B is reduced with respect to T_A and a ' phase results. Quantitative analysis of these effects will follow elsewhere.

3.4. Coexistence and competition between phases

More can be understood about the phase diagram figure 2 having argued for the " phases. N''_{II} and N''_{III} differ in the sign of the small order parameter S_A . Returning to the potential U_A (2.2) governing the behaviour of S_A (see (2.10)) one sees that the coefficient of $P_2(z)$ changes sign at a volume fraction

$$\bar{\chi} = (xv_C - v_f) / [x(v_C - v_A S_A / S_B)] \tag{3.4}$$

inducing a change of sign in S_A at roughly this point. Putting in values for figure 2 one obtains from this crude estimate $\bar{\chi} = 0.166$, in agreement with the phase boundary found from calculation. That the N''_{II} / N''_{III} phase line is nearly vertical follows from the smallness of S_A . In (3.4) the only temperature dependence of $\bar{\chi}$ comes from the S_A / S_B factor. If $|S_A| \sim 0$ then this term in the denominator can be neglected and $\bar{\chi}$ is temperature independent. An exactly analogous analysis from U_B gives the same conclusion about the steepness of the $N'_{III} - N'_I$ boundaries (see figures 3(a) and 5, where $|S_B| \sim 0$). This argument can be refined (Renz 1986) to show that the phase lines are exactly vertical.

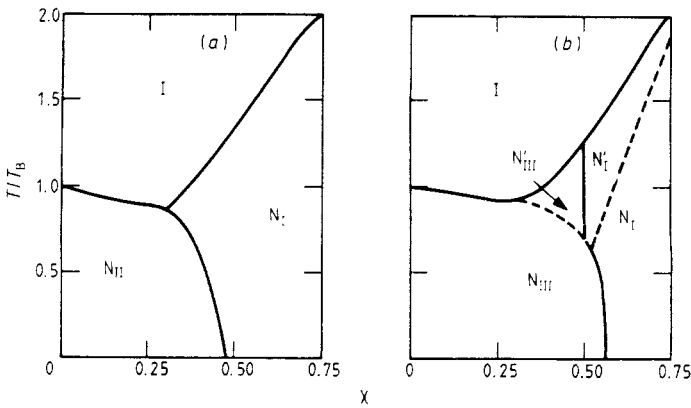


Figure 5. The effect of changing side-main chain coupling. Phase diagrams with reduced temperature T/T_B against volume fraction of side chain χ in the allowed range 0 to 0.75 corresponding to the side chain axial ratio $x=3$. In (a) the coupling constants $v_a : v_b : v_c : v_f : \epsilon / l_{seg}$ are in the ratio 3 : 2 : 1 : 3 : 2. In (b) the coupling between main and side chains, v_c , is doubled to $v_c = 2$. The effect is to remove the N_{II} phase in favour of the N''_{III} phase.

The factors governing the sign of the coefficient of P_2 in U_A (equation (2.2)), evident through (3.4), and in U_B (equation (2.3)) crudely control the coexistence between the unprimed phases as well. This was seen in the interpretation of N_{III} existence as $\chi \rightarrow 0$ in figure 2. We examine, in figure 5, the consequences of doubling the main chain/side chain nematic coupling v_C while keeping all other factors constant. In figure 5(a) the weaker coupling means that the hinge prevails and an N_{II} phase with $S_A \leq 0$ results. In figure 5(b), with twice the value of v_C , N_{III} results ($S_A \geq 0$). This same competition between nematic field ($\sim xv_c$) and hinge (v_f) was evident from the discussion for figure 3(a) where the balance was changed by the variation of x rather than v_c .

3.5. Apparently anomalous optical properties

The combs of figure 5(a) are also interesting because they show an N_{II} - N_I -I sequence of transitions which form an illustration of the unusual variation of optical anisotropy one could expect. In figure 6 the system of figure 5(a) has its variation of order parameters displayed as a function of reduced temperature at a fixed side chain volume fraction $\chi = 0.4$. The exchange of signs of S_A and S_B at $T/T_B = 0.6$ could give misleading variations of optical properties in the assignment of phase type. Imagine initially that χ , S_A^- and S_B^- (the order parameters on the lower side of $T = 0.6$) and the molecular optical anisotropies $\Delta\alpha_A$, $\Delta\alpha_B$ are such that the anisotropy measured in the laboratory is zero:

$$\Delta\alpha^- = (1 - \chi)\Delta\alpha_B S_B^- + \chi\Delta\alpha_A S_A^- = 0. \tag{3.5}$$

Above the transition, using (3.5), one has for the optical anisotropy

$$\Delta\alpha^+ = \chi\Delta\alpha_A S_A^+ [1 - (S_B^+/S_B^-)(S_A^-/S_A^+)] \tag{3.6}$$

where each of the order parameter ratios is negative and of modulus less than unity, and so the sign of $\Delta\alpha^+$ is determined by $\Delta\alpha_A$ only. This crude example, which ignores

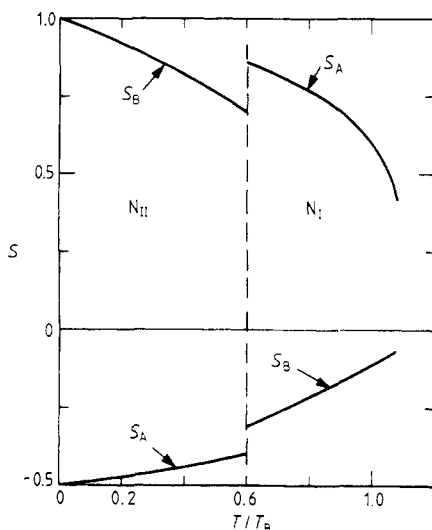


Figure 6. The combs of figure 5(a) at volume fraction $\chi = 0.4$ showing the transitions N_{II} - N_I -I. This involves the exchange in signs of the order parameters at a reduced temperature of $T/T_B = 0.6$ with possibly unusual consequences for such properties as optical anisotropy (see text).

internal field corrections, is merely to show that unusual effects such as optical anisotropies increasing with temperature can be envisaged. The converse situation to (3.5) could also arise, namely that $\Delta\alpha^+$ could be zero or very small and the N_{II} - N_I transition would then be confused with a transition to an I state. Of course an NMR experiment, measuring one of the order parameters only, would be unambiguous in its identification of a mesophase, except when the probe were to be on a component in a primed or double primed phase where the order parameter is very small.

4. Discussion

We conclude by summarising what we have calculated and discuss its relation to experiment.

In common with other problems in polymer liquid crystals, that of nematic combs involves a competition between the entropy of the semi-flexible main chain, and the drive toward orientational order of the main and side chains. We introduced five antagonistic influences and as a consequence derived three different types of nematic phases. Our aim was to elucidate the various possibilities for order and the transitions between options. To that end we did not try to estimate the various coupling constants introduced, but rather took certain combinations demonstrating the different types of phase behaviour. These types illustrate the outcome of the competition between the side and main chains. The oblate phase, N_I , where the main chain explores the plane perpendicular to the director is new, and the other two prolate cases N_{II} and N_{III} where the main chain is on average along the director have certain similarities with the backbone (non-comb) polymers discussed previously. Their ordering and the interplay between main and side chains is apparently new. Subtleties such as the exchange of sign of the order parameters of the components, apparently anomalous variation of optical properties and re-entrant phases will complicate the experimental identification of such possibilities.

The distinction between the mesogenic behaviour of the teeth of the comb and their simple nematic counterparts rests in their lack of independence from the main chain arising from their connection via a hinge. Kock *et al* (1985) demonstrate this main-side chain coupling by photoelastic experiments on networks comprised of comb molecules. Firstly, a change in stress at constant strain occurs when $T = T_{N_I}$. The change in optical anisotropy is large compared with that induced by straining the isotropic network, indicating that side chains (with their high molecular anisotropy of polarisability) are ordering. Because of hinge coupling, main chains alter their conformations and there is a change in the natural dimensions of the network, explaining the stress change. Secondly, networks are observed to have large negative stress-optical coefficients, in contrast to their small positive values when the side chains are absent, indicating strongly hinged side chains possibly of the N_{II} type being negatively biased with respect to the strain axis.

Stress-optical measurements, where refractive indices along different axes in a network vary with applied stress, can identify the character of a phase. With a hinge consisting of $(CH_2)_4$ groups a positive photoelastic coefficient when $T > T_{N_I}$ indicates that side chains are parallel to the main chain. Below T_{N_I} this coefficient remains positive which, combined with x-ray evidence, indicates an N_{III} phase. Shortening the hinge to $(CH_2)_3$ produces a nematic phase, possibly optically negative and possibly the N_{II} phase. As Kock *et al* note, the phases have one axis defined by the uniaxial

nematic order and, when stress is applied perpendicular to this axis, another defined by the strain just as in the stress-optical response of a conventional network. The networks consequently become biaxial. The transition from N_{III} to N_{II} behaviour on shortening the hinge is plausible from our theoretical analysis.

Finkelmann and Wendorff (1985) discuss poly(methacrylate) combs with strong hinges $[(CH_2)_2]$ which in an undiluted melt exhibit negative uniaxial optical anisotropy. This suggests the N_{II} phase, but we recall our discussion before (2.2) regarding the induction of bottle brushes when side chains are close packed and have strong hinges. The concern is that the molecule simply becomes a huge rod and orders in the manner of conventional nematic rods. It is found, however, that the addition of as little as 5% of simple nematic solvent, identical to the teeth of the comb, is sufficient to destroy this optically negative state. If rods are very long it is known that considerable dilution is required before their nematic order is destroyed. Perhaps by altering the balance between interside chain coupling (effectively changing χ) and hinge effects, one is inducing such a phase change with the solvent, as predicted in § 3. Small angle scattering experiments on main chain dimensions in this solution, or stress-optical measurements on such networks subsequently swollen by nematic solvent, would elucidate the details of this phase change.

The N_I phase has certainly been seen by scattering experiments determining the radius of gyration of the main chain in directions parallel and perpendicular to the director (Kirste and Ohm 1985). In fact, the variation of chain dimensions is a possible universal phenomenon, independent of precise values taken for coupling constants, provided they are such as to force one into the appropriate phase. Examples of this were given in w_{GB} and w_w where backbone nematics were argued to have an exponential temperature variation of dimension parallel to the director, a consequence of the competition between chain bending, entropy and nematic ordering. We expect the N_{II} and N_{III} phases to have this characteristic at low enough temperatures. Atactic combs will possibly offer the best possibility of achieving this limit. For the new oblate case (2.22), (2.23) and (2.24) describe the corresponding variation of dimensions as the chain is compressed down toward a disk shape. To see exactly what (2.22) and (2.23) imply we reassemble (2.6) for Δ^2 , recalling that $\alpha = D^{-1}/l$ is the number of segments per effective step length. We then obtain

$$\Delta^2 = -3D^{-1}\beta[(1-\chi)v_B S_B - (v_i/n - \chi v_C)S_A]/2l \quad (4.1)$$

where for the simpler one-component case ($\chi = 0$, no side chain) Δ^2 reduces to $-3D^{-1}\beta s_B v_B/2l$ in agreement with w_{GB} (where v_B/l is written as a). Combining (2.22) and (4.1) and noting that as T becomes small S_A and S_B saturate and the square bracket of (4.1) is weakly T dependent, one obtains

$$\langle R_z^2 \rangle = \text{constant } TL_B \quad (4.2)$$

i.e. chains should shrink in a particularly simple manner as temperature is lowered. For $\langle R_\perp^2 \rangle$ we have a saturation value of $2L_B D^{-1}$ which, since $D^{-1} = 2\varepsilon/k_B T$ depends on temperature, will grow simply because the effective step length is becoming larger, rather than because the nature of the walk continues to change. The ratio of dimensions

$$\langle R_z^2 \rangle / \langle R_\perp^2 \rangle = 1/4\Delta^2 + O(\Delta^{-3}) \quad (4.3)$$

scales like T^2/ε at strong enough nematic ordering and hence depends on $\varepsilon(T)$ as well. Jähnig (1979) has argued for certain systems that ε is a weak function of temperature but this is unlikely to be a general phenomenon (he argued for cases

where the flexibility in the backbone came from $-\text{CH}_2-$ sequences). In such comb phases as N_I one probably has to look to the smectic phase with underlying N_I order to see more qualitative aspects of chain dimension-exponential (activated) variation (Renz and Warner 1986a). The experiments of Kirste and Ohm (1985) do not give a sufficient number of points for the resolved radii of gyration as a function of temperature to check (4.2).

One potential difference from Kirste and Ohm's analysis arises: they point out that biasing a Kuhn walk does not alter the total radius of gyration of a molecule (averaged over directions). They use this to explain their observation that in the N_I phase $\langle R^2 \rangle$ is unchanged from its value in the I phase. Resolving the components $\langle R_x^2 \rangle$ and $\langle R_\perp^2 \rangle$ (their definition of the latter differs from ours by a factor of two) and then averaging yields the same result as the powder averaged value $\langle R^2 \rangle$. In our worm-like chain picture this is mysterious. As we report in (2.22) and (2.23) and their subsequent discussion, in the frame of the nematic the result of compression toward a disk is that

$$\langle R_\perp^2 \rangle \equiv \langle R_x^2 + R_y^2 \rangle \rightarrow 2L_B D^{-1} \quad (4.4)$$

and $\langle R_z^2 \rangle \rightarrow 0$. Powder averaging over orientations θ of the disk normal, appropriate to the unaligned nematic sample, would yield $2L_B D^{-1} \langle \sin^2 \theta \rangle = \frac{4}{3} L_B D^{-1}$ for $\langle R_\perp^2 \rangle$. The average $\langle R^2 \rangle$ along a scattering vector squared would be $\frac{2}{3} L_B D^{-1}$, half of (4.4) since only one component of $\langle R_\perp^2 \rangle$ lies along the scattering vector. This is twice the value obtained from the Kuhn analysis and used by Kirste and Ohm. We stress that this holds when the nematic field is very strong and the polymer shape approaches that of a disk. In the initial stages below T_{NI} the nematic field is not so strong and $\langle R^2 \rangle$ will be closer to the isotropic value. Of course the fundamental model of a chain is closer to that of a worm and the Kuhn effective step length derives from the expression $\langle R^2 \rangle / L$. Our analysis indicates that the precise value of the Kuhn step length derived from comparison with the worm value of $\langle R^2 \rangle / L$ depends on the dimensionality of the random walk:

$$\begin{aligned} 3\text{D:} \quad & \langle R^2 \rangle / L = D^{-1} \rightarrow l = D^{-1} \\ 2\text{D:} \quad & \langle R^2 \rangle / L = 2D^{-1} \rightarrow l = 2D^{-1}. \end{aligned} \quad (4.5)$$

The conclusion is perhaps that it is dangerous to take a Kuhn model for a chain and expect it to have the same step length as one goes between dimensions.

Another point of divergence from the Kuhn picture arises in the N_{II} and N_{III} prolate phases. In those cases we argue that in the strong nematic limit the comb becomes rod-like. A Kuhn process where the steps are all aligned gives a three-fold increase in $\langle R_z^2 \rangle$ and no change in $\langle R^2 \rangle$ itself whereas a rod has $\langle R^2 \rangle$ greater by a factor of L/D^{-1} . The difference of course is that successive bonds are not only aligned with respect to the nematic director but changes in direction with respect to the previous bond are also penalised by the nematic, leading eventually to a rod.

The increase in $\langle R^2 \rangle$ for both prolate ($\Delta^2 < 0$) and oblate ($\Delta^2 > 0$) deviations of the worm from spherical conformation means that for $|\Delta|^2 \sim 0$ we must have $\langle \delta R^2 \rangle \sim \Delta^4$ for the change in mean-square dimension. Changes in the dimensions associated with each direction, $\langle \delta R_z^2 \rangle$ and $\langle \delta R_\perp^2 \rangle$, must be linear in Δ^2 since they change sign on going from oblate to prolate. Since in Kirste and Ohm's experiment $\langle \delta R_z^2 \rangle / \langle R^2 \rangle \sim \langle \delta R_\perp^2 \rangle / \langle R^2 \rangle \sim 10\%$ it is plausible to expect that $\langle \delta R^2 \rangle / \langle R^2 \rangle$ will be small, perhaps around 1%, and that greater degrees of anisotropy in R_z and R_\perp are required to see $\langle R^2 \rangle$ change. Predicted properties of combs, other than their qualitative phase structure and variation of dimensions, are not so universal. An example is the latent entropy

(equation (2.17)). For backbone systems ww found this to be a universal value, but here, where there are two components interacting, the same simplification does not occur. We can reduce (2.17) somewhat in the light of the coupling constant ratios introduced in § 3. After some algebra and using the expression $\alpha = D^{-1}/l$, the number of segments per effective step length, one obtains for the latent entropy per repeat unit

$$\Delta S/R = -\frac{3/(0.3878)^2}{(T_C/T_B)^2} \left(\frac{l}{D^{-1}}\right) [x\chi v'_A S_A^2 + n(1-\chi) S_B^2 + 2S_A S_B (n\chi v'_C - v'_f)] - \left(\frac{nl}{D^{-1}}\right) \lambda_0^{(c)} \quad (4.6)$$

where T_C/T_B is the reduced transition temperature of the figures and $\lambda_0^{(c)}$ is the eigenvalue at the transition. The components of the expression scale in understandable ways: the first factor with l/D^{-1} as an artefact of our reducing temperatures by T_B , the transition temperature of the pure system, which reduces to $\epsilon v_B/l$ times a constant. The second factor is $\lambda_0^{(c)}$, the free energy per step length of main chain, times the number of step lengths per repeat unit, nl/D^{-1} . As in the case of backbone latent entropies (ww), this places restrictions on ΔS since D^{-1} is separately determinable from a neutron scattering experiment for chain dimensions.

Acknowledgments

We are grateful for extensive discussions with Drs J M F Gunn and R C Ball. Dr W Renz's communication about limits to the stability of this mean field theory and about the precise structure of phase diagrams is gratefully acknowledged. XJW acknowledges the hospitality of the Rutherford Appleton Laboratory during the execution of this research.

References

- de Gennes P G 1982 *Polymer Liquid Crystals* ed A Ciferri, W R Krigbaum and R B Meyer (New York: Academic) p 115
- Engel M, Hisgen B, Keller R, Kreuder W, Beck B, Ringsdorf H, Schmidt H-W and Tschirner P 1985 *Pure Appl. Chem.* **57** 1009
- Faber T E 1977 *Proc. R. Soc. A* **353** 247
- Finkelmann H and Wendorff H J 1985 *Polymer Liquid Crystals* ed A Blumstein (New York: Plenum) p 295
- Gunn J M F 1985 Private communication
- Hornreich R M 1985 *Phys. Lett.* **109A** 232
- Jähnig F 1979 *J. Chem. Phys.* **70** 3279
- 1981 *Mol. Cryst. Liq. Cryst.* **63** 157
- Kirste R G and Ohm H G 1985 *Makromol. Chem. Rapid Commun.* **6** 179
- Kock H J, Finkelmann H, Gleim W and Rehage G 1985 *Polymer Liquid Crystals* ed A Blumstein (New York: Plenum) p 275
- Maier W and Saupe A 1959 *Z. Naturf.* **14a** 882
- Meixner J and Schäffe F M 1954 *Mathieuische Funktionen und Sphäroidfunktionen* (Berlin: Springer)
- Renz W 1986 Private communication
- Renz W and Warner M 1986 *Phys. Rev. Lett.* **56** 1268
- ten Bosch A, Maissa P and Sixou P 1983a *Phys. Lett.* **94A** 299
- 1983b *J. Chem. Phys.* **79** 3462
- Wang X J and Warner M 1986a *J. Phys. A: Math. Gen.* **19** 2215
- 1986b *RAL report* 86-036
- Warner M and Flory P J 1980 *J. Chem. Phys.* **73** 6327
- Warner M, Gunn J M F and Baumgärtner A 1985 *J. Phys. A: Math. Gen.* **18** 3007
- Wojtowicz P J and Sheng P 1974 *Phys. Lett.* **48A** 235